Electromagnetic resonances in linear and nonlinear optics: phenomenological study of grating behavior through the poles and zeros of the scattering operator

M. Nevière and E. Popov*

Laboratoire d'Optique Electromagnétique, Unité de Recherche Associée au Centre de la Recherche Scientifique No. 843, Faculté des Sciences de Saint-Jérôme, Case 262, 13397 Marseille Cedex 20, France

R. Reinisch

Ecole Nationale Supérieure d'Electronique et de Radioelectricité de Grenoble, Laboratoire d'Electromagnétisme, Microondes et Opto-électronique, Unité de Recherche Associée au Centre de la Recherche Scientifique No. 833, B.P. 257, 38016 Grenoble Cedex, France

Received May 10, 1994; revised manuscript received September 22, 1994; accepted September 26, 1994

The poles and zeros of the scattering operator of a corrugated waveguide and of a bare grating are studied mathematically and numerically. An initial tutorial section recalls how their use can explain grating anomalies and other curious phenomena in linear optics. This approach is then used in nonlinear optics to understand and predict curious efficiency-curve shapes observed in the study of second-harmonic generation and optical bistability enhanced by a corrugated surface.

1. INTRODUCTION

When Wood discovered grating anomalies in 1902,[1] they were so named because they appeared as a strange and unexplained phenomenon. Wood was indeed astounded to see that under special illumination conditions the grating efficiency in a given order dropped from maximum to minimum illumination, the ratio being approximately 10 to 1, within a wavelength range not greater than the distance between the sodium lines. Lord Rayleigh[2] was the first to try to explain these abrupt variations by connecting them to the passing off of higher orders. Although a historical review of all the experimental and theoretical studies that were devoted to the understanding of Wood's anomalies is beyond the scope of this paper, we point out that Fano[3] was the first to suggest that anomalies could be associated with the excitation of a surface wave along the grating. The development[4] of the electromagnetic theory of gratings in the 1970's, which permitted accurate computation of grating efficiencies and of the scattering operator, has fully confirmed this explanation. After the research of Maystre and Nevière[5] and Nevière *et al.*,[6] it has been established that Wood's anomalies can be predicted and studied from the knowledge of the complex poles and zeros of the scattering (S) matrix, the poles being equal to the propagation constants of the leaky surface waves that may exist in the vicinity of the grating surface. Other strange phenomena can be studied along the same lines; examples are total absorption of light by a metallic grating and coupling of an incident laser beam into a waveguide,[7] and, in addition, perfect blazing of a corrugated waveguide near a second-order stop band.[8] Thus this technique is becoming more and more popular among grating theoreticians[9] and is termed pology. Indeed, simply the knowledge of the complex poles of the determinant of the S matrix, and eventually of the complex zeros of some of its elements, allows one to account for complicated shapes of grating anomalies and brings physical insight into the various above-mentioned strange phenomena, which a mere numerical computation does not bring.

In addition to the physical insight brought by such a phenomenological study, another important point is that the resonant excitation of a leaky surface wave near a grating, which occurs when a suitable phase matching between the incident plane wave and the guided wave is achieved, leads to a strong enhancement of the field near the grating surface.[10] This effect, which is already interesting in the linear optics domain for topics such as near-field microscopies,[11] can become even more interesting in nonlinear optics when the field enhancement acts with a power ≥ 2. Thus nonlinear effects, which are usually weak, can be increased by several orders of magnitude[12] and can become important; among them are Raman scattering, second-harmonic generation, luminescence, the Kerr effect, and optical bistability. It is the aim of this paper to show that pology contributes significantly to the understanding of complicated behaviors of some of these nonlinear phenomena. In order to demonstrate that, we first present the basic principles of pology in linear optics.

2. POLOLOGY IN LINEAR OPTICS

Figure 1 shows the notation used in grating theory. The grating surface, $y = g(x)$, divides space into regions ① and ② with refractive indices ν_1 and ν_2. When an incident plane wave with circular frequency ω, TE or TM polarized, falls upon the grating under incidence θ, it produces a field $u(x, y)$ that, outside the modulated region de-

0740-3232/95/030513-11$06.00

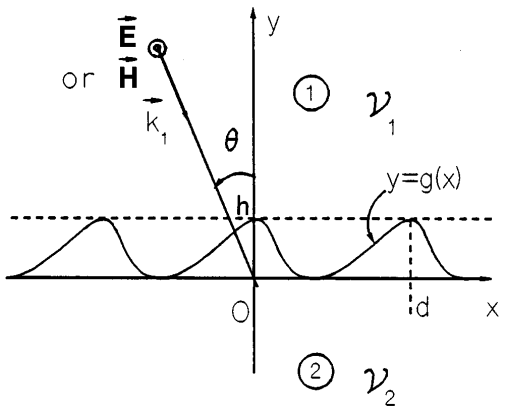

Fig. 1. Schematic representation of a grating, with notation.

fined by $0 \le y \le h$, can be represented by superpositions of plane waves, called Rayleigh expansions[4]:

If $y > h$,

$$u(x, y) = A_0 \exp[i(\gamma_0 x - \beta_0 y)] + \sum_{n=-\infty}^{+\infty} B_n \exp[i(\gamma_n x + \beta_n y)]. \quad (1)$$

If $y < 0$,

$$u(x, y) = \sum_{n=-\infty}^{+\infty} T_n \exp[i(\gamma_n x - \beta'_n y)], \quad (2)$$

where

$$\gamma_n = k_1 \sin\theta + nK, \quad (3)$$

$$K = \frac{2\pi}{d},$$

$$\beta_n = \sqrt{k_0^2 \nu_1^2 - \gamma_n^2} \quad \text{or} \quad i\sqrt{\gamma_n^2 - k_0^2 \nu_1^2}, \quad (4)$$

$$\beta'_n = \sqrt{k_0^2 \nu_2^2 - \gamma_n^2}, \qquad \mathrm{Re}(\beta'_n) + \mathrm{Im}(\beta'_n) > 0, \quad (5)$$

$$k_0 = \omega/c,$$

where d denotes groove spacing.

A. Definition of the Scattering Matrix

Let P be the number of diffracted propagating plane waves for a given angle θ and $U(\theta)$ be the set of corresponding values of n. Let us then consider the general case in which a set of P incident plane waves of the form $A_n \exp(-i\beta_n y)\exp(i\gamma_n x)$, with $n \in U(\theta)$, fall upon the grating. For $y > h$, they generate P diffracted plane waves of the form $B_n(\theta)\exp(i\beta_n y)\exp(i\gamma_n x)$ and an infinity of evanescent waves. In linear optics, if we are given A_n, the Rayleigh coefficients $B_n(\theta)$ of the diffracted waves are determined in a unique manner and depend on A_n linearly.

There are several ways to define a scattering matrix that links the incident field to the diffracted one. The simplest way is to write

$$B_n(\theta) = \sum_{m=-\infty}^{+\infty} S_{nm}(\theta) A_m \quad (6)$$

for any value of n and m from $-\infty$ to $+\infty$. Equation (6) defines what will be called the large scattering matrix, $S(\theta)$, which permits determination of both propagating and evanescent orders from the given incident field. For those who are not interested in evanescent orders, Eq. (6) can be replaced by

$$B_n(\theta) = \sum_{m \in U(\theta)} s_{nm}(\theta) A_m, \quad (6')$$

which defines the small-scattering matrix, $s(\theta)$. For lossless media such as perfectly conducting metals, it is sometimes useful to change Eq. (6′) into

$$B_n(\theta)\beta_n^{1/2} = \sum_{m \in U(\theta)} s'_{nm}(\theta) A_m \beta_m^{1/2}. \quad (6'')$$

This definition of another small scattering matrix, $s'(\theta)$, has the advantage of leading to a matrix that has symmetry properties[13] and unitarity, because it operates on vectors whose squared norms are diffracted energy. However, for many questions studied in this paper, the definition given by Eq. (6) will be the simplest one and will suffice.

B. Resonance Phenomenon

When we study the response of a grating to an incident plane wave, θ, $\sin\theta$, and the product $\delta = \nu_1 \sin\theta$ are real numbers. Thus the S matrix is, for the physicist, a function of a real variable (θ or δ). However, it is instructive to try to answer the purely mathematical problem: If we allow δ to be a complex variable, does the S matrix present complex poles and/or complex zeros in the complex-δ plane? This question may seem distasteful to experimentalists, which are concerned only with the $\mathrm{Re}(\delta)$ axis, but existence of complex poles not far from this real axis may explain interesting phenomena when δ is varied in its physical range of interest. Rewriting Eq. (6) in matrix form with δ dependences of the various matrices, we obtain

$$[B(\delta)] = [S(\delta)][A], \quad (7)$$

where $[B(\delta)]$ is a column vector with elements $B_n(\delta)$ and a similar definition applies to $[A]$. Inverting Eq. (7) gives

$$[A] = [M(\delta)][B(\delta)], \quad (8)$$

with $[M] = [S^{-1}]$, which, when no incident wave falls upon the grating, reduces to

$$[M][B] = 0. \quad (9)$$

We then get what is usually called the homogeneous problem,[7] which may lead to a nonzero solution only if

$$\det[M(\delta)] = 0. \quad (10)$$

Equation (10) may have complex solutions, and, for such a complex value of δ, Eq. (1) leads to a field that, for $y > h$, propagates along a direction close to the x axis and is attenuated in a direction perpendicular to it. A similar situation is found for $y < 0$; hence the solution of the homogeneous problem is called a leaky surface wave. The important point is to remember that propagation constants δ of such surface waves are complex numbers that are the zeros of $\det[M]$. Inverting matrix $[M]$ leads

to $S_{nm} = \|M_{mn}\|/\det[M]$, where $\|M_{mn}\|$ denotes the matrix formed from the minors of $[M]$.

The result is that the zero of $\det[M]$ is a pole of all the elements of the S matrix and thus of $\det[S]$. Hence it will be called δ^P in what follows. Equation (6) or (7) shows that all elements B_n of vector $[B]$ present the same complex pole δ^P, regardless of whether their index n belongs to $U(\theta)$, i.e., regardless of whether they have a propagating or an evanescent nature when an incident plane wave falls upon the grating.

Let us now go back to the situation in which a plane wave strikes the grating under incidence θ. Of course $\delta = \nu_1 \sin\theta$, which is real, cannot be equal to δ^p. But if, as happens for metallic gratings, $\mathrm{Im}(\delta^p) \ll 1$, δ becomes close to δ^p if the incidence is chosen in such a way that $\delta = \mathrm{Re}(\delta^p)$. Then S_{nm} are, of course, not infinite but culminate to a value inversely proportional to $\mathrm{Im}(\delta^p)$. Near this particular incidence, Eq. (6) or (7) leads to

$$B_n(\delta) = \sum_{m=-\infty}^{+\infty} \frac{C_{nm}(\delta)}{\delta - \delta^p} A_m , \tag{11}$$

where $C_{nm}(\delta)$ are slowly varying functions without pole, if we assume the nonmultiplicity of δ^p. Equation (11) can be approximated in a narrow range of incidence whose extension is of the order $\mathrm{Im}(\delta^p)$ by

$$B_n(\delta) \approx \frac{C}{\delta - \delta^p} ; \tag{12}$$

introducing $\delta^p = \delta'^p + i\delta''^p$, we get

$$|B_n(\delta)|^2 \approx \frac{|C|^2}{(\delta - \delta'^p)^2 + (\delta''^p)^2} . \tag{13}$$

Hence the moduli of *all* Rayleigh coefficients present a resonance phenomenon, governed by a Lorentzian curve centered around δ'^p, with half-width at half-maximum equal to δ''^p. Of course, this resonant behavior may be completely hidden if, in addition to a pole, $S_{nm}(\delta)$ presents a zero, as may occur for propagating orders whose energy is bounded by a conservation law. But evanescent orders that are not affected by this argument all present resonance lines simultaneously when θ is varied in such a way that $\nu_1 \sin\theta \approx \delta'^p$.

As soon as we have at our disposal efficient grating theories that permit computation of the S or the M matrix, the determination of δ^p can be done along the following lines. First, as soon as δ, and thus γ, is allowed to be complex, the definition given by Eq. (4) does not define β_n in a unique way. As shown in Ref. 7, it has to be replaced by an equation similar to Eq. (5), which includes a cut in the complex plane:

$$\beta_n = \sqrt{k_0^2 \nu_1^2 - \gamma_n^2} , \qquad \mathrm{Re}(\beta_n) + \mathrm{Im}(\beta_n) > 0 .$$

Second, the periodicity of the grating surface results in the multiplicity of poles δ^p, each of them having been derived from the central one by addition or subtraction of λ_0/d (Ref. 7). But, when groove depth h tends toward zero, all the determinations vanish except the one that tends to the propagation constant of the surface wave supported by the plane interface (surface plasmon–polariton or guided wave). Since the latter value can be determined in a straightforward or at least a simple way, it may be used as the starting point of an iterative process that looks for the different values of δ^p when h is increased from zero to its final value. Thus the loci of δ^p in the complex-δ plane can be obtained when an arbitrary grating parameter (e.g., h) is varied. Of course, this process requires a continuity hypothesis, which is broken when some of the cuts are crossed by the loci of δ^p.

C. Existence of Complex Zeros of $B_n(\delta)$

Since δ^P is common to all elements of the S matrix, relation (12) can be rewritten, including the groove-depth dependence, as

$$B_n(\delta, h) = \frac{u(\delta, h)}{\delta - \delta^p(h)} , \qquad u[\delta^p(h), h] \neq 0 .$$

In the limit case of a plane surface, all the amplitudes B_n vanish, except B_0, which tends toward the Fresnel reflection coefficient r; thus we get

$$B_0(\delta, 0) = r(\delta) = \frac{u(\delta, 0)}{\delta - \delta^p(0)} ,$$

from which we derive

$$u(\delta, 0) = [\delta - \delta^p(0)] r(\delta) .$$

The result is that, at the limit $h \to 0$, $\delta^p(0)$ not is only a pole for $B_0(\delta, 0)$ but is also a zero. When h increases from zero, of course things are changed. But continuity arguments imply that, at least for low grating modulation, a complex zero associated with the complex pole exists; it will be denoted $\delta^z(h)$. Its existence can easily be established for a perfectly conducting grating supporting only the zero diffracted order. For a diffracted efficiency equal to unity, whatever the incidence may be, to be found, a complex zero $\delta^z(h)$ equal to $\overline{\delta^p(h)}$ must be associated with the pole $\delta^p(h)$, if it exists. Here too, when losses are introduced into the metal, continuity arguments show that for good reflectors a complex zero $\delta^z(h)$, no longer equal to but close to $\overline{\delta^p(h)}$, still exists.

If the grating supports several diffracted orders, $B_0(\delta, h)$ near the resonance anomaly can be described intuitively by the sum of two terms, the first of which tends to the Fresnel reflection coefficient when $h \to 0$ and the resonant one of which is associated with the excitation of a surface wave:

$$B_0(\delta, h) = C(h) + \frac{D(h)}{\delta - \delta^p(h)} , \tag{14}$$

where

$$\lim_{h\to 0} C(h) = r(\delta) , \qquad \lim_{h\to 0} D(h) = 0 .$$

From Eq. (14) we deduce that

$$B_0(\delta, h) = C(h) \frac{\delta - \delta^p(h) + D(h)/C(h)}{\delta - \delta^p(h)}$$

or

$$B_0(\delta, h) = C(h) \frac{\delta - \delta^z(h)}{\delta - \delta^p(h)} , \tag{15}$$

with

$$\delta^z(h) = \delta^p(h) - D(h)/C(h) . \tag{16}$$

The conclusion is that any Rayleigh coefficient that corresponds to an order that does not vanish when the groove depth vanishes [$C(0) \neq 0$] must present a complex zero $\delta^z(h)$ associated with $\delta^p(h)$.

It it important to note that the above-mentioned argument does not apply to the minus-first order for which $C(h) = 0$. However, following a suggestion of Maystre (Université de Saint-Jérome, Marseille, France), we can demonstrate at least in one particular case that B_{-1} must also present a zero. To that end, we choose a perfectly conducting grating that supports two diffracted orders, and we consider the $[s']$ scattering matrix defined by Eq. (6″). The poles $\delta^p(h)$ of det$[S]$ that also are poles of all S_{nm} elements are thus poles of s'_{nm} and of det$[s']$. But the unitarity of this matrix implies that det$[s']$ also has zeros that are equal to $\overline{\delta^p}$. Thus det$[s']$ can be written as

$$\det[s'] = C_d(\delta - \overline{\delta^p}),$$

where C_d depends on δ. Moreover, from Eqs. (6″) and (15) we derive

$$s'_{0,0} = C_{0,0}(\delta - \delta^z_{0,0}),$$

and the same reasoning when $A_0 = 0$ and $A_{-1} \neq 0$ leads to

$$s'_{-1,-1} = C_{-1,-1}(\delta - \delta^z_{-1,-1}).$$

Recalling that $\det[s'] = s'_{-1,-1}s'_{0,0} - s'_{0,-1}s'_{-1,0}$, we obtain

$$C_{-1,-1}(\delta - \delta^z_{-1,-1})C_{0,0}(\delta - \delta^z_{0,0}) - C_d(\delta - \overline{\delta^p}) = s'_{0,-1}s'_{-1,0}.$$

This shows that the product $s'_{0,-1}s'_{-1,0}$ is a second-degree polynomial of δ. Thus it has two zeros δ^z_ζ and δ^z_η and can be put into the form $s'_{0,-1}s'_{-1,0} = q(\delta - \delta^z_\zeta)(\delta - \delta^z_\eta)$. Reciprocity and unitarity[13] show that $s'_{0,-1}$ and $s'_{-1,0}$ play similar roles, and thus each of them has a complex zero. Since $B_{-1} = s'_{-1,0}A_0$, the zero of $s'_{-1,0}$ is also a zero of B_{-1}.

We end this section by pointing out that the definition of the scattering matrix can be extended to transmission gratings[14] and that existence of poles and zeros of the transmitted Rayleigh coefficients can be understood along the same lines.

D. Loci of $\delta^p(h)$ and $\delta^z(h)$ in the Complex-δ plane

Having established the existence of poles and zeros of the S-matrix determinant or elements, we show in Fig. 2 an example of their evolution in the complex-δ plane when groove depth h increases from zero. Starting from a common value near the real axis equal to $\delta^p(0)$ [with Im $\delta^p(0) > 0$], which is the propagation constant of the plane air–silver-interface plasmon, the pole and the zero separate and go toward parts of the complex plane when h increases. As soon as silver presents losses, δ^z and δ^p cannot be complex conjugates. But since these losses are small at 0.5-μm wavelength, the trajectories of poles and zeros are almost symmetrical. The diffracted energy remaining bounded, δ^p can never be real; i.e., its trajectory cannot cross the Re(δ) axis, and it goes toward the positive imaginary part of the complex-δ plane. On the other hand, δ^z goes toward the opposite direction, i.e., it crosses the real axis for a critical value h_c of h equal to 0.021 μm. For that particular groove depth, the grating of Fig. 2, if illuminated under incidence given by $\sin\theta = \mathrm{Re}(\delta^z)$, which has a wavelength-to-groove-spacing ratio large enough to diffract only the zeroth order, will absorb in totality the incident power.

Figure 3 shows the same trajectories for a dielectric coated grating used in TE polarization, when the dielectric film thickness e is increased. This time the curves start

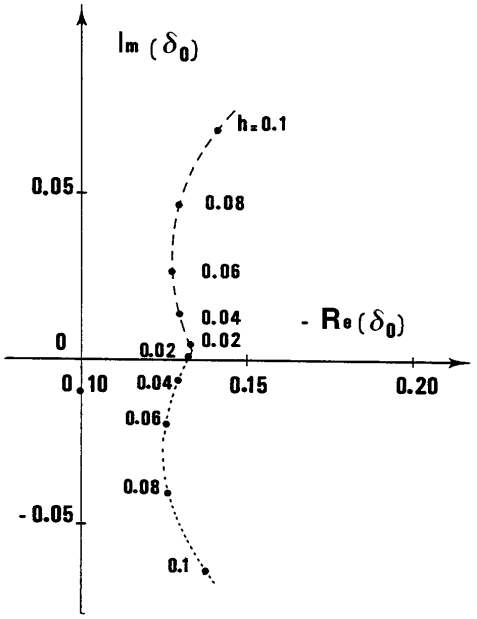

Fig. 2. Loci of the pole δ^p and the zero δ^z of $B_0(\delta, h)$ in the complex plane when h (in micrometers) is varied, for a 2400-groove/mm sinusoidal silver grating used in TM polarization. $\lambda = 0.5\,\mu$m. Long-dashed curve, δ^p; short-dashed curve, δ^z.

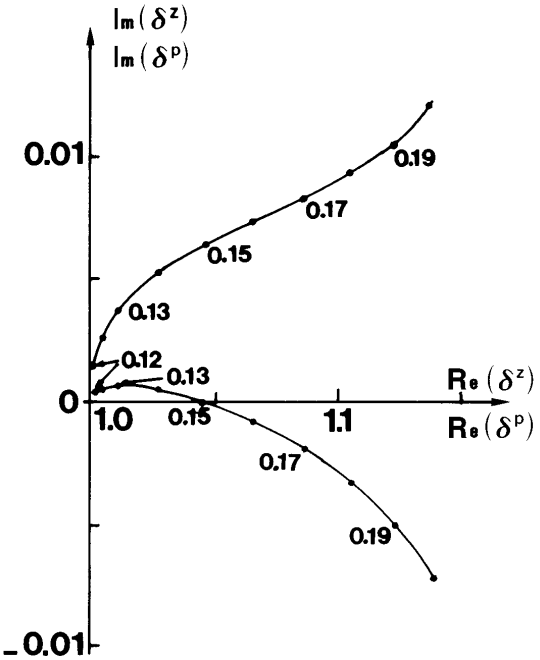

Fig. 3. Loci of the pole δ^p (upper curve) and the zero δ^z (lower curve) in the complex plane for a 2400-groove/mm, 10°22′ blaze angle aluminum grating used in TE polarization, at $\lambda = 0.492\,\mu$m. The grating is coated with a layer of MgF_2 with thickness e chosen as the parameter (in μm).

from the propagation constant of a lossy guided wave and again go toward opposite halves of the complex-δ plane. A total absorption phenomenon occurs for a suitable dielectric thickness.[15]

As soon as the existence of a pole and a zero has been established, including the slow dependence of $C(h)$ on δ in Eq. (15), the function $B_0(\delta, h)$ may be written as

$$B_0(\delta, h) = w(\delta, h)\,\frac{\delta - \delta^z(h)}{\delta - \delta^p(h)}, \tag{17}$$

where $w(\delta, h)$ is a complex regular function near δ^z and δ^p and does not present any zero in their vicinity. The study of the asymptotic behavior of the two terms of Eq. (17) shows that $\lim_{h\to 0} w(\delta, h) = r(\delta)$. Since $w(\delta, h)$ is a slowly varying function, Eq. (17) may be approximated by

$$B_0(\delta, h) \approx r(\delta)\,\frac{\delta - \delta^z(h)}{\delta - \delta^p(h)}\cdot \tag{17'}$$

Hence the following phenomenological formula is obtained for the zeroth order efficiency $\mathcal{E}_0$:

$$\mathcal{E}_0(\delta, h) = |B_0|^2 = R(\delta)\,\frac{|\delta - \delta^z(h)|^2}{|\delta - \delta^p(h)|^2}, \tag{18}$$

where $R(\delta)$ is the reflection factor of the energy. As soon as δ^z and δ^p are known, $\mathcal{E}_0(\delta, h)$ can be obtained immediately. It is worth noticing that, on the curves of Figs. 2 and 3, when the parameter h or e is increased, the pole and the zero move while their real parts are kept almost equal. It follows that when $\delta = \mathrm{Re}(\delta^p)$, $\mathcal{E}_0$ presents a minimum value close to $R(\delta)[\mathrm{Im}(\delta^z)/\mathrm{Im}(\delta^p)]^2$ derived from Eq. (18).

Figure 4 shows the efficiency curves derived, through Eq. (18), from the values of the poles and zeros plotted in Fig. 2. It is clear that for the critical value $h_c = 0.021\ \mu$m a phenomenon of total absorption is found. This has been thoroughly confirmed by experiments.[15,16]

On other periodic structures such as corrugated waveguides, the pole and the zero may have real parts that significantly differ. The zeroth-order efficiency curve then presents a more complicated shape with both a minimum [corresponding to $\mathrm{Re}(\delta^z)$] and a maximum [corresponding to $\mathrm{Re}(\delta^p)$] (Fig. 5). Here, too, phenomenological formula (18) fully accounts for this complicated shape and gives predictions in agreement with rigorous calculations. Under special circumstances, e.g., if the groove spacing is chosen in such a way that a surface wave is excited under near-normal incidence, or for a dielectric coated grating that supports both a guided wave and a plasmon, two complex poles and two complex zeros may be located at neighboring positions in the complex-δ plane. It is then straightforward[17] to extend phenomenological formula (18) by including all poles and zeros, and it has been verified[17] by rigorous calculations that the extended formula still gives an excellent prediction of the grating behavior.

3. POLOLOGY IN NONLINEAR OPTICS

A. Second-Harmonic Generation

When a high-power laser beam with circular frequency ω falls upon a grating, in addition to the diffraction phenomenon at ω, it generates, through a nonlinear interaction, a nonlinear polarization $\boldsymbol{\mathcal{P}}^{\mathrm{NL}}(2\omega)$ inside the grating material. This dipole collection radiates a field at 2ω circular frequency, which is itself diffracted by the grating. Since nonlinear effects are usually weak, it is generally assumed that the 2ω field does not interact with the field at ω. We thus make the usual undepleted-pump approximation, which allows us to study the second-harmonic generation by a grating through a three-step theory.[18,19] As a first step we determine the ω-diffracted field $\boldsymbol{\mathcal{E}}(\omega)$ by computing the corresponding scattering matrix $S(\omega)$. Second, we determine $\boldsymbol{\mathcal{P}}^{\mathrm{NL}}(2\omega)$, which depends on the grating material as well as on the polarization of light. In the case of a nonlinear dielectric, for example, we have

$$\boldsymbol{\mathcal{P}}^{\mathrm{NL}}(2\omega) = \chi(2\omega) \vdots \boldsymbol{\mathcal{E}}(\omega)\boldsymbol{\mathcal{E}}(\omega), \tag{19}$$

where χ is the third-order nonlinear susceptibility tensor. In the third step Maxwell equations plus boundary conditions at 2ω circular frequency lead to a linear diffraction

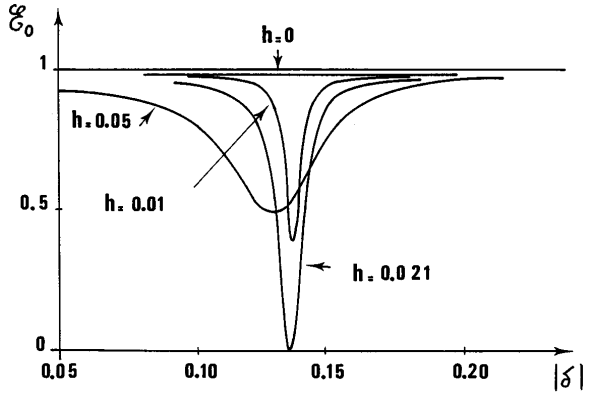

Fig. 4. Zeroth-order efficiency curves for several groove depths of a 2400-groove/mm sinusoidal silver grating as function of δ. $\lambda = 0.5\ \mu$m, TM polarization.

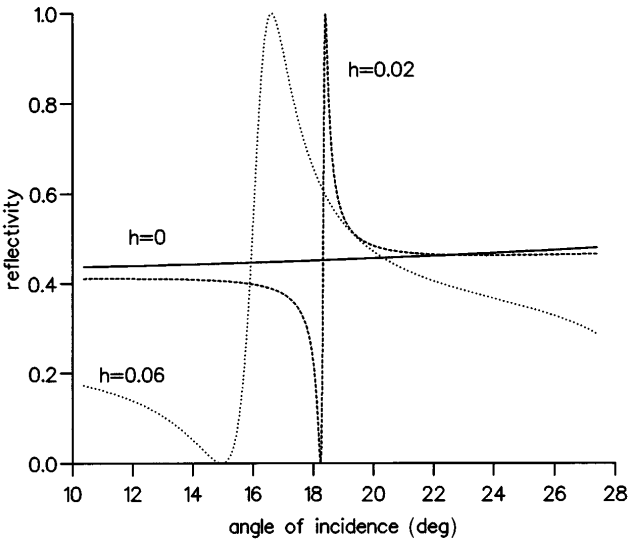

Fig. 5. Zeroth-order efficiency of a sinusoidal corrugated waveguide with thickness 0.19 μm ($\nu_1 = 1$, $\nu_2 = 2.3$, $\nu_3 = 1$) and $d = 0.37\ \mu$m, illuminated at $\lambda = 0.6328\ \mu$m, in TE polarization, as a function of incidence. The values of groove depths are given in micrometers.

problem in which $\mathcal{P}^{NL}(2\omega)$ acts as source term. It is then possible to define a scattering matrix at 2ω that links the diffracted field $\mathcal{E}(2\omega)$ to the source term $\mathcal{P}^{NL}(2\omega)$:

$$\tilde{B} = \tilde{S}(2\omega)\tilde{A}. \tag{20}$$

As in the linear part, $\tilde{B}$ is a vector whose components are the Rayleigh coefficients $\tilde{B}_n$ of the field (this time at 2ω frequency). Concerning the link between $\tilde{A}$ and $\mathcal{P}^{NL}$, its particular form depends on the method used to resolve the 2ω boundary value problem. It may include a numerical[18] or an analytical[19] integration with respect to the y coordinate inside the nonlinear region. But, in any case, this link is linear as far as the undepleted-pump approximation can be assumed.

The obvious consequence of linear equation (20) is that if $\mathcal{P}^{NL}(2\omega)$ has a pole, so does $\tilde{A}$ and, from Eq. (20), $\tilde{B}$, as well. If the ω field has a pole δ^p, called δ_1^p in what follows, Eq. (19) then shows that δ_1^p is a double pole of $\tilde{A}$ and $\tilde{B}$. Moreover, $\tilde{S}(2\omega)$ defined in Eq. (20) may also present a pole called δ_2^p. The result is that any component $\tilde{B}_n(2\omega)$ of $\tilde{B}$ will present three poles, a double one equal to the pole δ_1^p of $S(\omega)$ and a single one (δ_2^p) coming from $\tilde{S}(2\omega)$.

As is true in the linear regime, intuitive reasons can be found to predict the existence of associated complex zeros that come from unitarity in the case of lossless media and continuity arguments. Moreover, the argument developed in Subsection 2.C [see Eqs. (14) and (15)] allows us to predict the existence of three different zeros associated with the zeroth diffracted order at 2ω.

Indeed, the associated plane device that we obtained by letting h tend toward zero already presents a nonzero nonlinear Fresnel reflection coefficient r^{NL}. Then, for $h \neq 0$, $\tilde{B}_0(\delta, h)$ can be written as a nonresonant term plus the resonant one:

$$\tilde{B}_0(\delta, h) = \tilde{C}(h) + \frac{\tilde{D}(h)}{[\delta - \delta_1^p(h)]^2[\delta - \delta_2^p(h)]}, \tag{21}$$

where

$$\lim_{h\to 0} \tilde{C}(h) = r^{NL}(\delta), \qquad \lim_{h\to 0} \tilde{D}(h) = 0.$$

Equation (21) can immediately be rewritten as

$$\tilde{B}_0(\delta, h) = \frac{\tilde{C}(h)\delta^3 + a\delta^2 + b\delta + c}{[\delta - \delta_1^p(h)]^2[\delta - \delta_2^p(h)]}, \tag{22}$$

where a, b, and c depend on h but are independent of δ. The third-order polynomial at the numerator thus has three complex zeros, δ_1^z, δ_2^z, and δ_3^z. The conclusion is that the presence of a nonresonant term in Eq. (21) results in the existence of three different zeros associated with the three poles.

It is worth noticing that, in general, the double pole δ_1^p is associated not with a double zero but with two different ones, namely, δ_1^z and δ_3^z, δ_2^z being the zero associated with the simple pole δ_2^p. When $h \to 0$, $\tilde{B}_0(\delta, h) \to \tilde{C}(0) = r^{NL}(\delta)$. Then Eq. (22), rewritten as

$$\tilde{B}_0(\delta, h) = \tilde{C}(h)\frac{(\delta - \delta_1^z)(\delta - \delta_3^z)(\delta - \delta_2^z)}{(\delta - \delta_1^p)^2(\delta - \delta_2^p)}, \tag{23}$$

shows that, since there is no resonant behavior for the plane device, $\lim_{h\to 0} \tilde{D}(h) = 0$, the numerator must tend toward the denominator. The result is that two of the zeros (δ_1^z and δ_3^z) tend toward the double pole δ_1^p, and the third zero tends toward δ_2^p:

$$\lim_{h\to 0} \delta_1^z(h) = \delta_1^p = \lim_{h\to 0} \delta_3^z(h), \qquad \lim_{h\to 0} \delta_2^z(h) = \delta_2^p.$$

Another interesting way to obtain the same result is explained in Appendix A, with the same argument used as in Subsection 2.C.

A more physical insight can be proposed to prove the existence of complex zeros. If we generalize to nonlinear optics the reasoning that led to Eq. (14), we are, indeed, led to represent $\tilde{B}_0(\delta, h)$ by the sum of four different terms:

$$\tilde{B}_0(\delta, h) = a' + \frac{b'}{(\delta - \delta_1^p)^2} + \frac{c'}{\delta - \delta_2^p} + \frac{d'}{(\delta - \delta_1^p)^2(\delta - \delta_2^p)}, \tag{21'}$$

where a', b', c', and d' depend on h but not on δ.

The first term, a', is the off-resonant one. The second term is the resonant term at the pump frequency, the third term is the resonant term at the signal frequency, and the last term is the resonant term at both ω and 2ω frequencies when phase matching occurs. The use of Eq. (21′) instead of Eq. (21) leads to the same Eq. (22) with different values for coefficients a, b, and c. Thus the conclusion regarding the existence of three complex zeros is identical. As soon as the existence of poles and zeros in nonlinear optics is established, their numerical values as well as their loci in the complex-δ plane when an arbitrary parameter is varied can be determined along the same lines as in linear optics with the computer code based on the three-step theory of Ref. 19.

In what follows, we deal with two types of nonlinear corrugated system. The first one is a nonlinear corrugated waveguide that supports TE waveguide modes. Its upper boundary is corrugated, and its lower one is flat [Fig. 6(a)]. The second system consists of a nonlinear dielectric layer deposited upon a silver grating [Fig. 6(b)], which supports the surface plasmon. The pump wavelength is equal to 1.06 μm, and the corrugation is sinusoidal with period $d = 0.4$ μm in both cases. The nonlinear properties of the middle layers are characterized by a single nonzero component of the nonlinear susceptibility tensor:

$$\chi_{xxx} = \varepsilon_0 \qquad \text{for the } 2\omega \text{ TM case},$$
$$\chi_{zzz} = \varepsilon_0 \qquad \text{for the } 2\omega \text{ TE case}.$$

The substrate of the dielectric waveguide has refractive index $\nu_3(\omega) = 1.7$, $\nu_3(2\omega) = 1.905$. The cladding is air, and the waveguide nonlinear material has indices with small losses: $\nu_2(\omega) = 2 + i0.0005$, $\nu_2(2\omega) = 2.01 + i0.0005$, and thickness e equal to 0.58 μm.

Figure 7(a) presents the trajectories of the poles and the zeros of the zeroth reflected orders at 2ω, when the groove depth of the grating is varied. Without corrugation two of the zeros merge into one of the poles (which is a double pole). This double pole corresponds to a waveguide mode at pumping frequency ω. The other couple of zero and pole corresponds to the waveguide mode at 2ω. With increasing groove depth two phenomena can

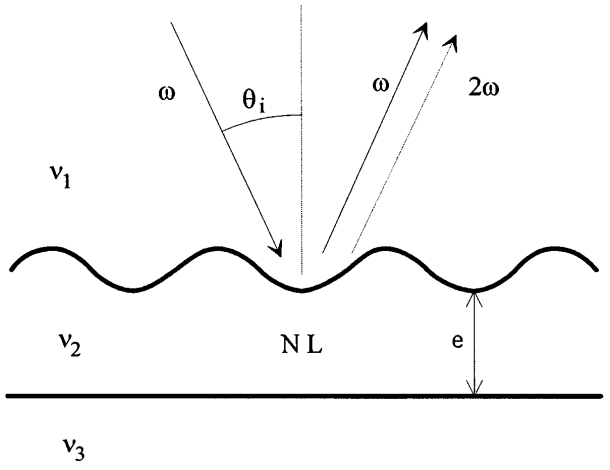

(a)

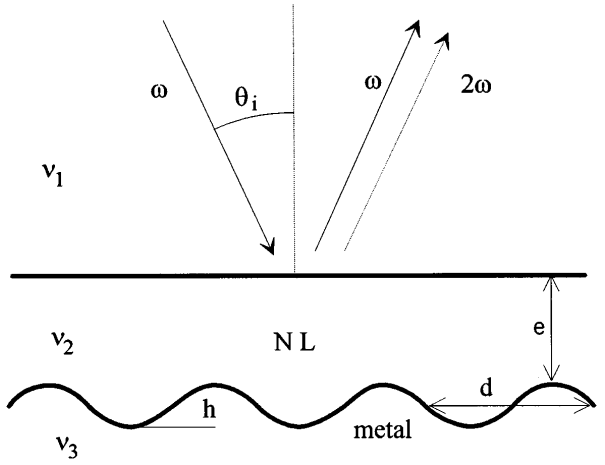

(b)

Fig. 6. Cross-sectional view of the two corrugated systems with a nonlinear middle layer: (a) modulation of the upper interface, (b) modulation of the lower interface. NL, nonlinear polarization.

be observed. At first the poles and the zeros become separated, so that resonance anomalies appear at both ω and 2ω frequencies. Second, the real parts of the poles get closer, so that at $h = 0.12$ μm the three poles almost coincide. This means that for $h = 0.12$ μm the phase-matching condition[20] is fulfilled. The zeros are far away: two of them have quite different real parts, and the third one has an imaginary part much larger than the imaginary parts of the two other poles. A high resonance peak is observed in the angular dependence of specularly reflected order at 2ω [Fig. 7(b)]. The phenomenological approach [Eq. (23)] gives the same dependence, provided that the correct values of the poles and the zeros plotted in Fig. 7(a) are used. Notice that the right-hand scale is different from the left-hand one because in the phenomonological approach we have taken $\tilde{C} = 1$. When the latter is properly normalized, not only the shape of the phenomonological approach curve but also its absolute values become equal to the values obtained from rigorous computation. The normalization can be performed in different ways. The best way is to use the rigorous maximum value. Another possibility is to use for $\tilde{C}$ the value of the second-harmonic reflectivity of the corresponding flat surface.

The second example [Fig. 6(b)] has a silver substrate with refractive index $\nu_3(\omega) = 0.226 + i6.9863$, $\nu_3(2\omega) = 0.129 + i3.25$. The upper medium is homogeneous, with refractive index $\nu_1 \equiv \nu_2$: $\nu_1(\omega) = 1.534$, $\nu_1(2\omega) = 1.414$. An artificial layer with thickness $e = 0.01$ μm is assumed to have nonlinear properties. The trajectories of the poles and the zeros [Fig. 8(a)] have behavior similar to that in Fig. 7(a), except for two peculiarities:

1. The imaginary parts of the poles differ significantly, owing to the different values of the losses at ω and at 2ω.
2. The zeros (except for δ_1^z) do not move far from the poles. This peculiarity determines the behavior of the efficiency (i.e., second-harmonic reflectivity). Contrary to

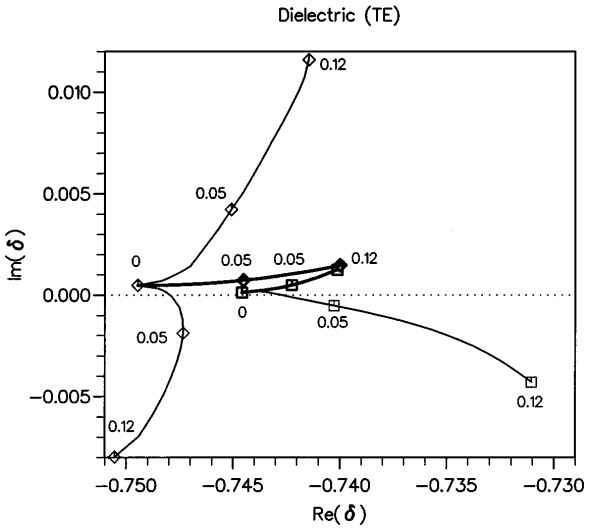

(a)

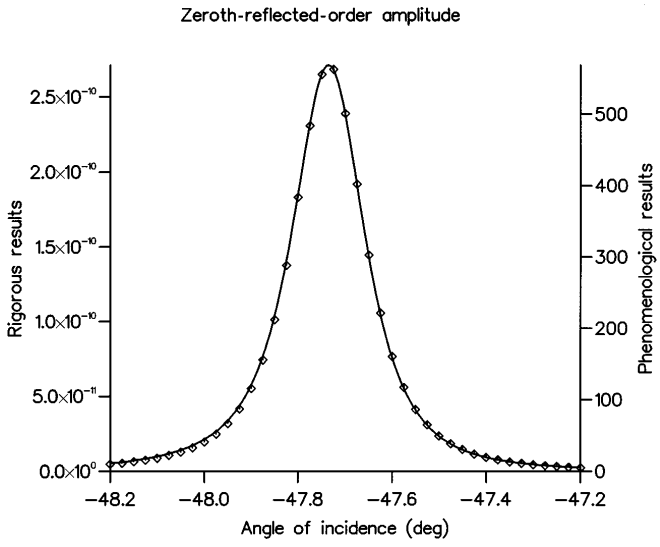

(b)

Fig. 7. (a) Trajectories of the poles (thick curves) and the zeros (thin curves) of the zeroth reflected order at 2ω for the system of Fig. 6(a), when the groove depth is varied. The values are given in micrometers. (b) The second-harmonic reflectivity as a function of angle of incidence in the region of waveguide-mode excitation. Solid curves, rigorous results; diamonds, phenomenological results from Eq. (23), with $\tilde{C} = 1$, $h = 0.12$ μm.

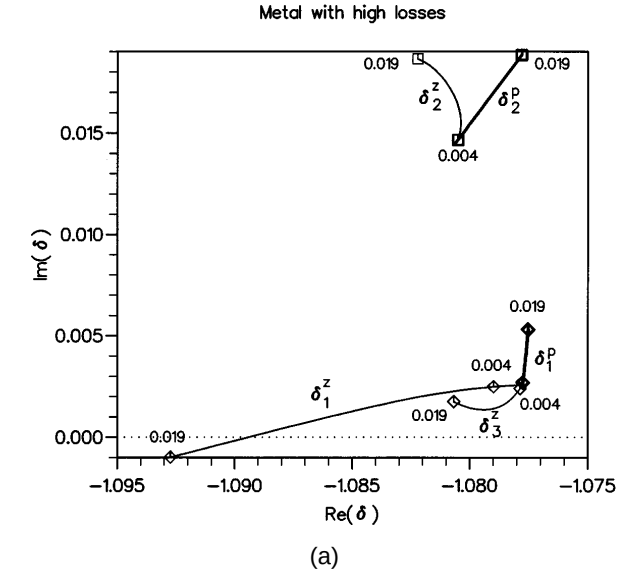

(a)

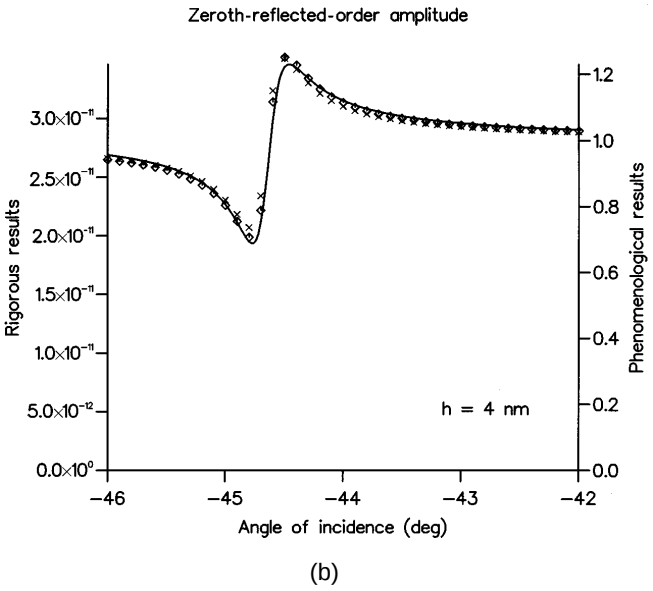

(b)

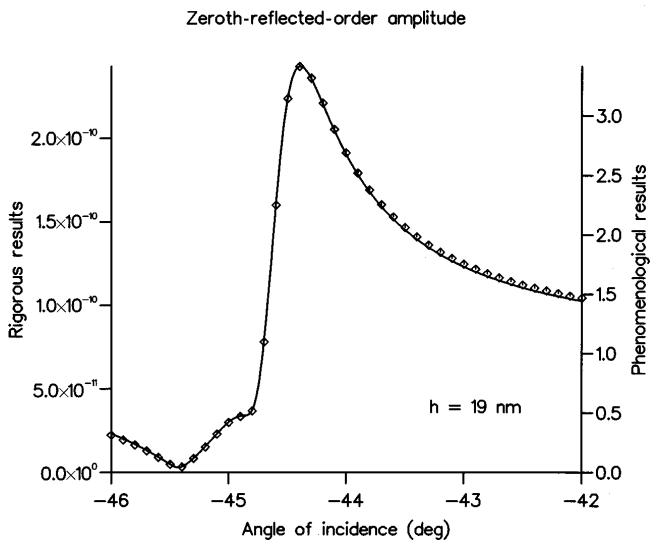

(c)

Fig. 8. (a) Same as in Fig. 7(a) but for the system of Fig. 6(b); (b), (c) nonlinear reflectivity as a function of angle of incidence for (b) $h = 0.004$ μm and (c) $h = 0.019$ μm. Solid curves, rigorous results; diamonds, phenomenological results from Eq. (23); crosses, phenomenological results with a single pole δ_1^p and a single zero δ_1^z.

the case of Fig. 7(b), where the angular dependence has a typical Lorentzian shape, now, in Fig. 8(b), the zeros that stay in the vicinity of the poles deform the shape of the resonance curve. When the grating is very shallow ($h = 4$ nm) two of the zeros almost coincide with two of the poles ($\delta_2^z \approx \delta_2^p$ and $\delta_3^z \approx \delta_1^p$), and the angular dependence is almost completely determined by a single pole (δ_1^p)–zero (δ_1^z) couple and Eq. (15) [crosses in Fig. 8(b)].

When $h = 0.019$ μm, the imaginary parts of two of the zeros (δ_1^z and δ_3^z) are smaller than the distances between zeros and poles, and zeros can be localized in the angular dependence as minima. There are three peculiarities in Fig. 8(c): a maximum near $-44.5°$, a minimum near $-45.5°$, and a step near $-44.8°$. The corresponding real parts of the zeros and poles are

$$\mathrm{Re}(\delta_1^z) \approx -1.093 = \nu_1(\omega)\sin(-45.44°),$$
$$\mathrm{Re}(\delta_3^z) \approx -1.081 = \nu_1(\omega)\sin(-44.8°),$$
$$\mathrm{Re}(\delta_1^p) \approx \mathrm{Re}(\delta_2^p) \approx -1.077 = \nu_1(\omega)\sin(-44.6°),$$

values that correspond quite well to the positions of the minimum and the maximum.

From Figs. 7 and 8 it is clear that pology enables one immediately to account for complicated, non-Lorenztian (or Lorenztian) shapes of second-harmonic resonance curves, provided that the complex values of both the poles and the zeros of the S matrix are known.

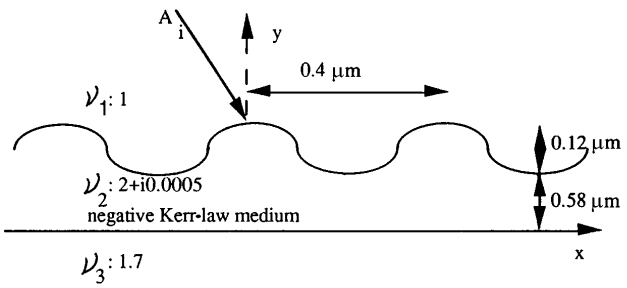

Fig. 9. Schematic representation of a bistable corrugated waveguide.

B. Kerr Effect and Optical Bistability

Let us now consider the corrugated waveguide represented in Fig. 9, which is filled with a Kerr-like medium. At high incident power, the refractive index of the waveguide becomes a function of the field intensity:

$$\nu_2^2 = \nu_{2,0}^2[1 + \alpha|E^2(x, y)|],$$

where the low-power value of ν_2 (equal to $\nu_{2,0}$) is given in Fig. 9 and α is the Kerr constant.

The main difference between the Kerr effect and second-harmonic generation is that in the Kerr effect the signal frequency is the same as the pump frequency. The Kerr effect modifies the refractive index only by one or a few percent, modifications that remain small compared with the refractive-index step at the boundaries. Thus the field distribution is only slightly modified, as is discussed below, contrary to what happens in second-harmonic generation, in which the nonlinearity is the only source for the 2ω field. That is why it is possible for the Kerr effect to derive the phenomenological parameters from the linear study. We are then able to derive a simple phenomenological formula that accounts for complicated hysteresis loops.

Let us first consider the linear problem ($\alpha = 0$). Equation (6), along with the existence of a pole and, for propagating orders, the existence of a zero of the S matrix, leads to

$$B_n = C_n \frac{\delta - \delta_n^z}{\delta - \delta^p} A_i, \tag{24}$$

where A_i is the incident amplitude and C_n is a slowly varying function near δ^p and δ_n^z. On the other hand, the amplitude A_{gw} of the guided wave inside the nonlinear dielectric can be written as

$$A_{gw} = \frac{t_p}{\delta - \delta^p} A_i, \tag{25}$$

where t_p is the incoupling coefficient of the guided mode. Thus Eq. (24) gives

$$B_n = C_n A_i + C_n \frac{\delta^p - \delta_n^z}{\delta - \delta^p} A_i = C_n A_i + g_n A_{gw}, \tag{26}$$

where

$$g_n = \frac{C_n}{t_p}(\delta^p - \delta_n^z).$$

The resolution of the rigorous boundary value problem in linear optics gives coefficients C_n, g_n, and t_p, which depend only on the transverse field map $E(0, y)$, whose shape in the vicinity of a resonance does not depend on δ in the linear regime. Thus C_n, g_n, and t_p are independent of δ in the linear regime.

In the nonlinear regime[20,21] δ^p becomes a function of A_i, denoted $\delta^{p,\mathrm{NL}}(A_i)$; so does δ_n^z, but because the Kerr constant α is small, ν_2^2 is only slightly changed, and the field map near a resonance is also only slightly changed. The result is that C_n and g_n remain the same as in the linear regime, and Eq. (26) can be replaced by

$$B_n^{\mathrm{NL}} = C_n A_i + g_n A_{gw}^{\mathrm{NL}}. \tag{26'}$$

From the equality of g_n, d_n, and t_p in linear and nonlinear regimes we get

$$C_n \frac{(\delta^p - \delta_n^z)}{t_p} = C_n \frac{(\delta^{p,\mathrm{NL}} - \delta_n^{z,\mathrm{NL}})}{t_p}.$$

Hence

$$\delta_n^{z,\mathrm{NL}} - \delta_n^z = \delta^{p,\mathrm{NL}} - \delta^p. \tag{27}$$

This equation shows that the curves describing the variations as functions of $(A_i)^2$ of $\mathrm{Re}(\delta_n^{z,\mathrm{NL}})$ and $\mathrm{Re}(\delta^{p,\mathrm{NL}})$, as well as those of $\mathrm{Im}(\delta_n^{z,\mathrm{NL}})$ and $\mathrm{Im}(\delta^{p,\mathrm{NL}})$, must be parallel curves. This prediction is confirmed for $n = 0$ in Fig. 10, which is obtained from rigorous computations[22] performed on the device shown in Fig. 9. Since for a Kerr-like guiding material ν_2^2 is real, only the real parts of $\delta_n^{z,\mathrm{NL}}$ and $\delta^{p,\mathrm{NL}}$ are changed when A_i is increased, the imaginary parts remaining constant. For photoabsorbing materials the situation should be vice versa.

The consequence of the parallelism of the trajectories of $\delta^{p,\mathrm{NL}}$ and $\delta_n^{z,\mathrm{NL}}$ is that poles and zeros can be expressed as

$$\delta^{p,\mathrm{NL}} = \delta^p + \xi_p|A_{gw}^{\mathrm{NL}}|^2, \qquad \delta_n^{z,\mathrm{NL}} = \delta_n^z + \xi_p|A_{gw}^{\mathrm{NL}}|^2,$$

where ξ_p can be calculated in terms of overlap integrals[23] from the coupled-mode analysis. Since the linear study

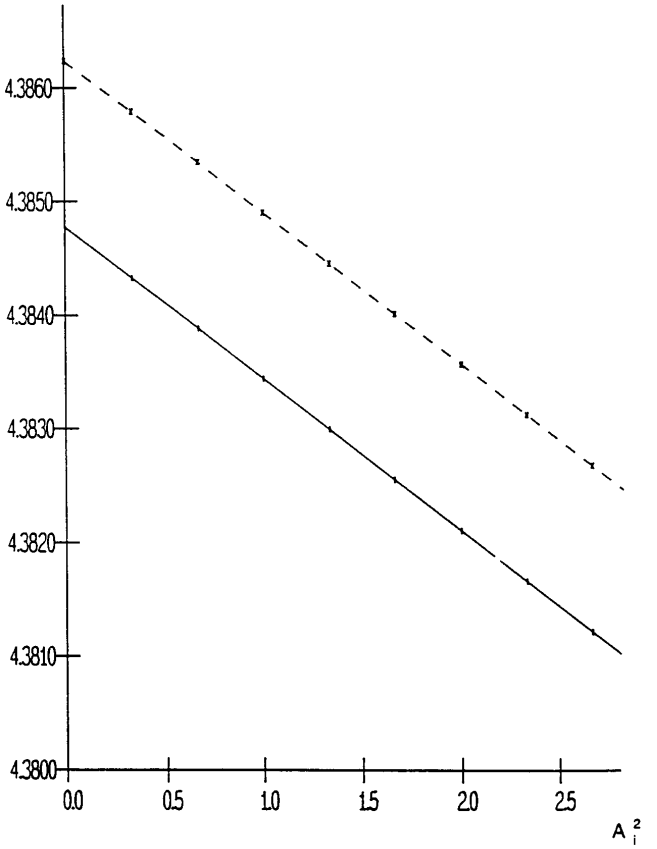

Fig. 10. Trajectories of the real parts of a pole (solid curve) and a zero (dashed curve) of the S matrix when A_i^2 is varied.

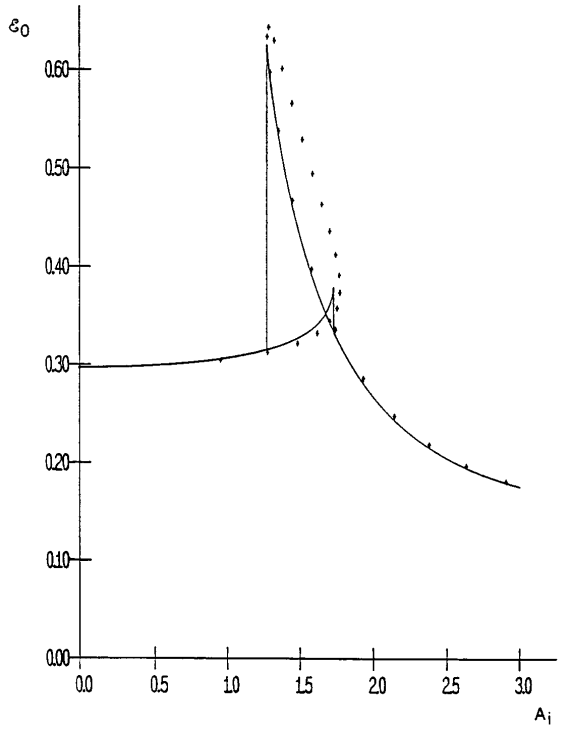

Fig. 11. Zeroth-order efficiency curve, $\mathcal{E}_0 = (B_0^{\mathrm{NL}}/A_i)^2$, as a function of A_i: solid curve, results of rigorous computation; crosses, results derived from Eqs. (25′) and (26′).

of gratings gives δ^p, δ_n^z, t_p, C_n, and g_n, both guided-wave amplitude and reflected-order amplitudes can be obtained through two simple formulas:

$$A_{gw}^{\mathrm{NL}} = \frac{t_p}{\delta - \delta^{p,\mathrm{NL}}} A_i \,, \tag{25′}$$

$$B_n^{\mathrm{NL}} = C_n A_i + g_n A_{gw}^{\mathrm{NL}} \,. \tag{26′}$$

Thus the nonlinear response of the device can be obtained without resolution of the nonlinear problem of diffraction. Figure 11 compares the prediction from Eqs. (25′) and (26′) with those coming from rigorous study.[22] It can be seen that even the complicated butterflylike shape of the curve is predicted by this simple analysis. Moreover, Eq. (26′) can be generalized to a beam with finite width[21] and accounts for the so-called transverse effects linked with spatial limitation of the incident wave.

4. CONCLUSION

The formalism of poles and zeros of the elements of the scattering operators, which was used many years ago to explain grating anomalies and other curious phenomena in linear optics, has been extended to the study of diffraction in nonlinear optics in the presence of electromagnetic resonances. The position of the zero(s) with respect to the pole(s) is an important parameter. Indeed,

- In the case of second-harmonic generation, a zero too close to a pole (relative distance close to the width of the resonance line) limits, and even decreases, the second-harmonic efficiency.
- For optical Kerr interactions, the position of the zero(s) with respect to the pole(s) permits understanding of the existence of exotic bistability loops.

Thus it can be seen that the knowledge of pole(s) and zero(s) constitutes powerful information when one is studying enhanced second-harmonic generation or optical bistability in the presence of electromagnetic resonances.

APPENDIX A

Let us write the zeroth Rayleigh coefficient in the linear or the nonlinear regime as the sum of a nonresonant term and a resonant one:

$$B_0(\delta, h) = C(\delta, h) + \frac{D(\delta, h)}{\mathcal{P}(\delta, h)} \,, \tag{A1}$$

where

$$\mathcal{P}(\delta, h) = 0 \qquad \text{for } \delta = \delta_n^p \,, \qquad n = 1, 2, 3, \ldots N \,,$$

$$\lim_{h \to 0} D(\delta, h) = 0 \,, \tag{A2}$$

$$C(\delta, 0) \neq 0 \,. \tag{A3}$$

In the range of δ that we are dealing with, $C(\delta, h)$ is assumed to have no zero. On the other hand, the zeros of $\mathcal{P}(\delta, h)$ induce resonant behaviors. Since such behaviors are never found for a plane device, it is assumed that $\lim_{h \to 0} D(\delta, h) = 0$.

Equation (A1) can be rewritten as

$$B_0(\delta, h) = C(\delta, h) \frac{\mathcal{R}(\delta, h)}{\mathcal{P}(\delta, h)} \,,$$

where

$$\mathcal{R}(\delta, h) = \mathcal{P}(\delta, h) + \frac{D(\delta, h)}{C(\delta, h)} \,.$$

At the limit of vanishing groove depth,

$$\lim_{h \to 0} \mathcal{R}(\delta, h) = \lim_{h \to 0} \mathcal{P}(\delta, h) = \mathcal{P}(\delta, 0) \,.$$

The result is that when $h \to 0$, the zeros of B_0 tend toward its poles, whatever the number of poles may be.

ACKNOWLEDGMENTS

The authors thank D. Maystre for helpful discussions; they also acknowledge the support of the European Community through the Brite–Euram Contract Flat Optical Antennas.

*On leave from the Institute of Solid State Physics, Bulgarian Academy of Sciences, 72 Trakia Boulevard, Sofia 1784, Bulgaria.

REFERENCES

1. R. W. Wood, "On a remarkable case of uneven distribution of light in a diffraction grating spectrum," Philos. Mag. **4,** 396–402 (1902).

2. J. W. S. Rayleigh, "Note on the remarkable case of diffraction spectra described by Prof. Wood," Philos. Mag. **14,** 60–65 (1907).
3. U. Fano, "The theory of anomalous diffraction gratings and of quasi-stationary waves on metallic surfaces (Sommerfeld's waves)," J. Opt. Soc. Am. **31,** 213–222 (1941).
4. R. Petit, ed., *Electromagnetic Theory of Gratings* (Springer-Verlag, Berlin, 1980).
5. D. Maystre and M. Nevière, "Sur une méthode d'étude quantitative des anomalies de Wood des réseaux de diffraction: application aux anomalies de plasmon," J. Opt. (Paris) **88,** 165–174 (1977).
6. M. Nevière, D. Maystre, and P. Vincent, "Application du calcul des modes de propagation à l'étude théorique des anomalies des réseaux recouverts de diélectrique," J. Opt. (Paris) **8,** 231–242 (1977).
7. M. Nevière, "The homogeneous problem," in *Electromagnetic Theory of Gratings*, R. Petit, ed. (Springer-Verlag, Berlin, 1980), pp. 123–157.
8. P. Vincent and M. Nevière, "Corrugated dielectric waveguides: a numerical study of the second-order stop bands," Appl. Opt. **20,** 345–351 (1979).
9. E. Popov, "Light diffraction by relief gratings: a macroscopic and microscopic view," in *Progress in Optics*, E. Wolf, ed. (Elsevier, Amsterdam, 1993), Vol. XXXI, pp. 139–187.
10. E. Popov and L. Tsonev, "Electromagnetic field enhancement in deep metallic gratings," Opt. Commun. **69,** 193–198 (1989).
11. D. W. Pohl and D. Gourjon, eds., *Near Field Optics*, Vol. 242 of NATO Advanced Sciences Institutes Series E (Kluver, Dordrecht, The Netherlands, 1993).
12. R. Reinisch, G. Vitrant, and M. Nevière, "Electromagnetic resonance induced nonlinear optical phenomena," in *Nonlinear Waves in Solid State Physics*, A. D. Boardman, N. Bertolotti, and T. Twardowski, eds. (Plenum, New York, 1990), pp. 435–461.
13. M. Nevière, M. Cadilhac, and R. Petit, "Applications of conformal mappings to the diffraction of electromagnetic waves by a grating," IEEE Trans. Antennas Propag. **AP-21,** 37–46 (1973).
14. E. Popov, L. Mashev, and D. Maystre, "Theoretical study of anomalies of coated dielectric gratings," Opt. Acta **33,** 607–619 (1986).
15. E. G. Loewen and M. Nevière, "Dielectric coated gratings: a curious property," Appl. Opt. **16,** 3009–3011 (1977).
16. M. C. Hutley and D. Maystre, "The total absorption of light by a diffraction grating," Opt. Commun. **19,** 431–436 (1976).
17. D. Maystre, M. Nevière, and P. Vincent, "On a general theory of anomalies and energy absorption of diffraction gratings and their relation with surface waves," Opt. Acta **25,** 905–915 (1978).
18. R. Reinisch and M. Nevière, "Electromagnetic theory of diffraction in nonlinear optics and surface-enhanced nonlinear optical effects," Phys. Rev. B **28,** 1870–1885 (1983).
19. E. Popov and M. Nevière, "Surface-enhanced second-harmonic generation in nonlinear corrugated dielectrics: new theoretical approaches," J. Opt. Soc. Am. B **11,** 1555–1564 (1994).
20. R. Reinisch, G. Vitrant, J. L. Coutaz, P. Vincent, M. Nevière, and H. Akhouayri, "Modal analysis of grating couplers for nonlinear waveguides," Nonlin. Opt. **5,** 111–118 (1993).
21. R. Reinisch, M. Nevière, P. Vincent, and G. Vitrant, "Radiated diffracted orders in Kerr-type grating couplers," Opt. Commun. **91,** 51–56 (1992).
22. P. Vincent, N. Paraire, M. Nevière, A. Koster, and R. Reinisch, "Gratings in nonlinear optics and optical bistability," J. Opt. Soc. Am. B **2,** 1106–1116 (1985).
23. H. Kogelnik, "Theory of dielectric waveguides," in *Integrated Optics*, T. Tamir, ed. (Springer-Verlag, Berlin, 1975), pp. 13–81.